Scientific Research Publishing

American Journal of Analytical Chemistry, 2023, 14, 451-466
https://www.scirp.org/journal/ajac
ISSN Online: 2156-8278
ISSN Print: 2156-8251

Y Zeolites Modified by Organosilane for Toluene Adsorption under High Humidity Condition

Boyu Zhang, Kuo Zhang, Ziqiang Duan, Jianping Zhu, Junan Gao*

State Key Laboratory of Chemical Resource Engineering, Beijing University of Chemical Technology, Beijing, China
Email: *gaojunan321@163.com

How to cite this paper: Zhang, B.Y., Zhang, K., Duan, Z.Q., Zhu, J.P. and Gao, J.N. (2023) Y Zeolites Modified by Organosilane for Toluene Adsorption under High Humidity Condition. *American Journal of Analytical Chemistry*, **14**, 451-466.
https://doi.org/10.4236/ajac.2023.1410026

Received: September 6, 2023
Accepted: October 28, 2023
Published: October 31, 2023

Abstract

Y zeolites have moderate microporous pore size, large specific surface area, and good hydrothermal stability, which were widely used in industrial adsorption of volatile organic compounds (VOCs), but the performance of Y zeolites in adsorption of VOCs under high humidity conditions is terrible. In this paper, Y zeolites with different silica-alumina ratios were hydrophobically modified by organosilane and characterized by XRD, FTIR, SEM, BET, NMR. In the experiments of static and dynamic adsorption of VOCs by modified Y zeolites, it can be concluded that the static water adsorption capacity of Y zeolites with silica-aluminum ratio of 5 and 40 after silica modification decreased by 62 wt% and 53 wt%, under the conditions of high humidity, GHSV = 15,000 h^{-1}, T = 35˚C and initial concentration of toluene C_0 = 5000 $mg{\cdot}m^{-3}$. The saturation adsorption capacity of toluene was increased from 0.06 $g{\cdot}g^{-1}$, 0.09 $g{\cdot}g^{-1}$ to 0.15 $g{\cdot}g^{-1}$, 0.21 $g{\cdot}g^{-1}$, the adsorption selectivity of Y zeolites for water was reduced and that for toluene was increased after Vapor phase silanization overlay modification. The present modification method might carry out targeted modification of zeolites surface, provide research ideas and guidance under high humidity conditions.

Keywords

Y Zeolites, Hydrophobic Modification, Volatile Organic Compounds, Toluene

1. Introduction

Volatile organic compounds (VOCs) come from transportation exhaust, industrial production processes, building decoration materials and waste incineration

processes, which are toxic irritating, even cause cancer [1]-[6]. Due to the limitations of production technology and development cost, source treatment is usually difficult to be applied practically, therefore, end-of-pipe treatment is an essential measure for the generated organic waste gases. Nowadays, VOCs end-of-pipe treatment technologies can be divided into two technologies: recovery and elimination, where elimination technologies are mainly catalytic combustion, photocatalysis, biodegradation and plasma methods, the recovery methods are mainly absorption, condensation, membrane separation, and adsorption [6]-[11]. Compared with other methods, adsorption method has incomparable advantages in the treatment of VOCs in large volume and low concentration, and it can be combined with incineration process to achieve deep purification of VOCs waste gas. Moreover, zeolites have good non-combustibility and high temperature regeneration compared to activated carbon commonly used in industry due to silica-aluminate skeleton and porous structure [12] [13]. the thermodynamic study of adsorption of various adsorbents revealed that at low concentrations of VOCs, the enthalpy of adsorption of all types of organics was the largest for Y zeolites. Its pore channels have the strongest adsorption force on organic molecules. Y zeolites have no obvious selective adsorption for different VOCs gases, and the equilibrium adsorption capacity is greater than other zeolites such as ZSM-5, filamentous zeolite, Beta zeolites and M41S. The structure of zeolite Y (FAU) has good permeability (the pore volume accounts for 50% of the total volume) [14]-[19], the pore is cage-shaped, and the pore size is large (7.4 Å), so VOCs can better reach the internal position of zeolite [20]. However, in practical industrial applications, VOCs gases were usually mixed with water molecules, especially in specific sites where the relative humidity is up to 80% RH, and the aluminum atom in the zeolites skeleton replaces the silicon atom, which makes the zeolites show strong negative electricity and the presence of surface hydroxyl groups, which makes it show a strong affinity for polar molecules in the performance of adsorption of VOCs. The gaseous water molecules strongly compete with VOCs molecules for adsorption, thus affecting the adsorption performance of the adsorbent [20]-[25].

The higher silica-alumina ratio of zeolites, the better the hydrophobicity has been demonstrated in the relevant literature [26]. At this stage, the silicon-aluminum ratio of directly synthesized nano-NaY zeolites was generally low and poorly hydrophobic. It is necessary to modify Y zeolites with dealuminum and supplement silicone or silane surface modification to improve hydrophobicity. The methods of dealuminization and silica modification of Y zeolites include high-temperature hydrothermal dealuminization, liquid-phase reaction with ammonium fluorosilicate, gas-phase dealuminization and silica modification, and organic coordination reaction, or a combination of both methods [27] [28]. The zeolites cells obtained by high-temperature hydrothermal method shrink significantly, and the non-skeletal aluminum trapped in the zeolites cells will migrate and enrich heavily on the grain surface, resulting in uneven aluminum distribution, which was often modified with acid treatment to obtain Y zeolites

with high silica-aluminum ratio [29]. The gas-phase and liquid-phase dealumination and silica supplementation methods can dealuminate zeolites in a wide range, and the structural integrity of the dealuminated samples maintains the original adsorption capacity without secondary mesoporous channels, but lead to the destruction of the lattice, resulting in a significant decrease in crystallinity and the generation of a large number of hydroxyl vacancies [30] [31]. In contrast to the de-alumination and silica modification that changes the zeolites skeleton structure, the surface modification of Y zeolites using silylation reagents does not affect the internal pore structure and overcomes the disadvantages of the internal surface modification method. Silane compounds are highly reactive and will react strongly with the hydroxyl groups on the surface of zeolites, and the hydrophobic alkyl functional groups in organosilylation reagents grafted onto the surface of zeolites reduce the water adsorption energy and increase the hydrophobicity, but the silylation modification will graft too long carbon chains and block the pore channels, which affect the zeolites adsorption capacity of VOCs [31]-[36]. In order to achieve hydrophobic modification of the zeolites surface without blocking the pore channels and maintaining the adsorption capacity of VOCs, the long-chain silica grafted on the silane surface can be transformed into hydrophobic SiO_2 nanocrystallets by gas phase-over silicon modification, which is the biggest innovation point in this study.

In this paper, HY5 and HY40 were hydrophobically modified with trimethylchlorosilane as the modifying reagent by Vapor phase silanization overlay modification, which made hydrophobic SiO_2 nanocrystals transcrystallize and grow on the surface of zeolites, avoiding the blockage of zeolite pore channels by grafting too long carbon chains, and preparing hydrophobic Y zeolites with good adsorption performance of VOCs. The conformational relationships were investigated by combining XRD, BET, NMR, FTIR and other characterization methods. Dynamic adsorption experiments were conducted to investigate the adsorption and removal of toluene before and after the modification of Y zeolites with different silica-aluminum ratios, and revealed the competitive adsorption mechanism of water and toluene on the modified zeolites adsorbent, provided a theoretical and technical basis for the industrial adsorption and removal of VOCs under moisture-containing conditions.

2. Materials and Methods

2.1. Experimental Materials

The materials for this experiment were HY5, HY40, (SiO_2: Al_2O_3 = 5.40), purchased from Nankai Catalyst Plant; trimethylchlorosilane ($(CH_3)_3SiCl$, 99%), toluene; deionized water. All materials were of nanlytical reagent grade and were used without any further purification.

2.2. Preparation of Adsorbent

Vapor phase silanization overlay modification: A certain amount of commercial

Y zeolites was weighed and ground to 40 - 100 mesh. 3 g of Y zeolites was placed in a quartz tube with an inner diameter of 2 cm, and then injected with 50 ml/min nitrogen, which was activated and pretreated at 550˚C for 2 h, and cooled to 250˚C. Then the mixture of trimethylchlorosilane and nitrogen was injected for 40 min, and the unreacted trimethylchlorosilane was removed by purge with nitrogen of 50 ml/min for 1 h. When the temperature was raised to 550˚C, 50 ml/min oxygen was added, and the reaction lasted for 1 h, so that the carbonsilyl group was oxidized to silicon dioxide covering the surface of the zeolites. Silica coated Y zeolites can be obtained. HYX (X = 5.40) means hydrothermally prepared Y zeolites, G-HYX (X = 5.40) means silylated modified Y zeolites, F-HYX (X = 5.40) means Vapor phase silanization overlay modified Y zeolites.

2.3. Characterization Methods

X-ray diffraction (XRD) tests were carried out on a Philips X' PertMPD X-ray powder diffractometer with CuKα rays, tube voltage of 40 kV, tube current of 30 mA, and scanning speed of 1˚/min.

The N_2 adsorption experiments were carried out on a Mirometrics ASAP 2010 adsorber, and the specimens were pretreated at 200˚ for 3 h. The specific surface area was calculated using the BET formula, and the pore volume and pore diameter were calculated using the BJH method.

Fourier transform infrared spectra (FTIR) were taken on a Bruker IFS88 infrared spectrometer, and the samples were prepared by KB r compression and self-supported slices, respectively.

Cross-polarization/magic angle rotation ^{29}Si NMR (^{29}Si CP/MAS NMR) spectra were taken on a Bruker MSL-400WB NMR instrument with tetramethylsilane (TMS) as a reference material.

Water contact angle: The static water contact angle of zeolites was measured by DSA30 optical contact angle tester from Krüss, Germany.

2.4. Adsorbent Test Method

All experiments were tested using the devices shown in **Figure 1**. The specific experimental process is as follows:

Static adsorption experiments: the static water adsorption (sw) and toluene adsorption (sn) of zeolites at a constant temperature of 35˚C for 24 h were determined according to the method of GB-T6287-1986, and the Y hydrophobicity index (Hn), Hn = sn/sw, was calculated to indicate the hydrophobicity of zeolites [20].

Dynamic adsorption experiments: simulating industrial VOCs adsorption conditions, HY-X (X = 5.40) and FHY-X (X = 5.40) were used to evaluate the toluene adsorption capacity at 0% and 60% relative humidity, The longer the adsorbent penetration time (the exhaust concentration reaches 5 wt% of the intake concentration) and saturation adsorption time (the exhaust concentration

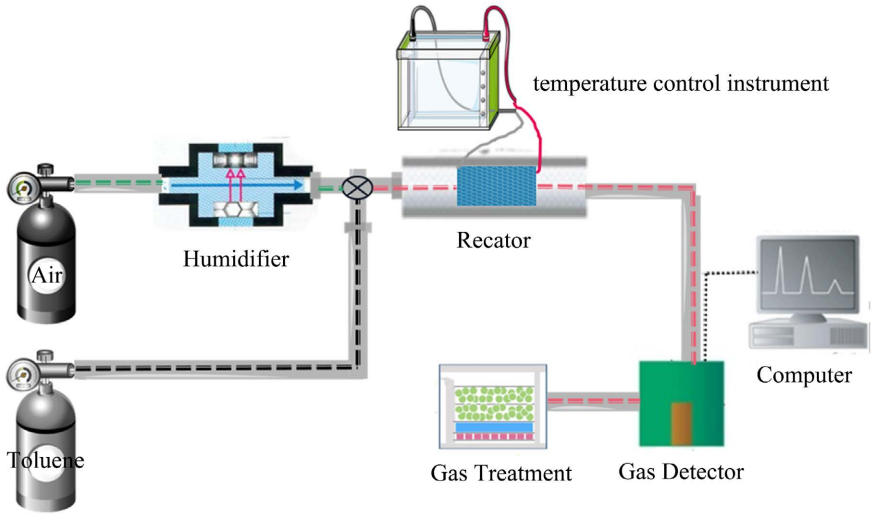

Figure 1. Toluene adsorption experimental setup.

reaches 100 wt% of the intake concentration), the greater the adsorption capacity. The whole adsorption system consists of generator, adsorption bed, detector, etc. [37]. N_2 was used as the carrier gas, and the gas containing a certain toluene concentration and relative humidity was simulated by adjusting and controlling the flow rate of the three gases into the adsorption device, and the toluene concentration in the exhaust gas was analyzed and determined by gas chromatograph. The zeolites samples were dried in a muffle furnace at 550˚C for 2 h to remove impurities in the adsorbent, and 5 g of sieved granular samples of 0.6 - 0.85 mm were loaded into the adsorption bed, and the adsorption tubes were placed in a constant temperature water bath at 35˚C for adsorption performance evaluation. The adsorption amount of toluene was calculated by integrating the adsorption curve, and the calculation formula was shown in Equation (1).

$$q = \frac{F \times c_0 \times 10^{-9}}{W}\left[t_s - \int_0^{t_s} \frac{c_i}{c_0} d_t\right] \quad (1)$$

Note: q: equilibrium adsorption amount, g/g; F: gas flow rate, ml/min; t-adsorption time, min; C_0 and C_i: mass concentration of toluene in the inlet gas and the tail gas after adsorption, mg/m^3; W: loading amount of adsorbent, g; t_s: adsorption equilibrium time, min.

3. Results and Discussion

Characterization of Adsorbent

Figure 2 shows the XRD spectrum before and after the modification of the sample, the crystal structure of the zeolites after silaneisation and gas phase overlapping silicon modification was basically complete. The peak type was sharp, the baseline was flat, and there was no impurity peak. The position of the main diffraction peak was offset, different degrees of cell contraction and the intensity of the diffraction peak decreases. Due to the high-temperature dealumination reaction

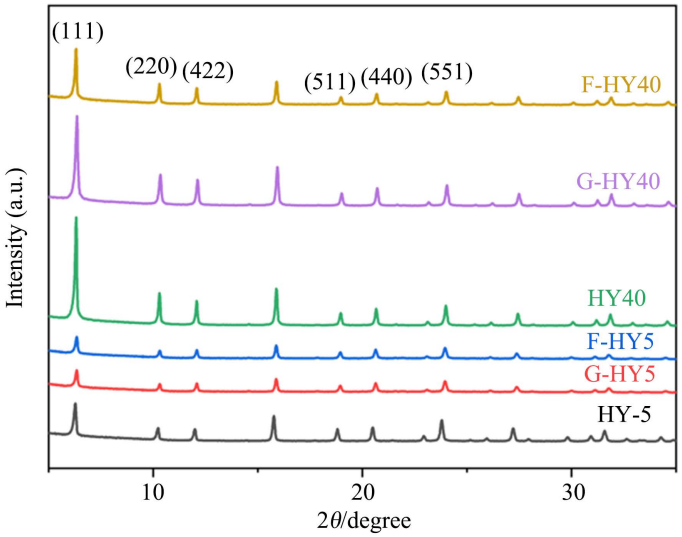

Figure 2. XRD diagram of Y zeolites.

of some Y zeolites skeleton aluminum and chloride ions in TMCS, which has caused the increase of lattice defects and the normalisation of zeolites pore structure, resulting in the decrease of the diffraction peak intensity. The diffraction peak at $2\theta = 6.2^{\circ}$ still appeared in the sample after Vapor phase silanization overlay modification, indicating that the layer spacing did not change significantly. It was assumed that the fumed silica modification successfully inserted amorphous silica into the interlayer of Y zeolites, and the conventional liquid-phase deposition Organosilanes modification of HY zeolites was easily affected by the uneven heat and mass transfer of the reaction material, resulting in agglomeration of grains, blockage of zeolites pore channels, and reduction of crystallinity and adsorption performance. According to the reaction mechanism of zeolites overlay silica modification, silanization had a directional mass transfer in the process of overlay silica reaction: partially pyrolyzed TMCs condensed with the silicon hydroxyl group on the surface of the Y zeolites, grafted on the surface of the zeolites, and the carbon silane group was oxidised to amorphous silica in the oxygen atmosphere and transferred to the surface and near the pore of the zeolites crystal to prepare modified HY with high crystallinity. This due to the gas phase in the reaction system, the concentration of carbon silane fragments in the gas stream was low and the contact area was large, sufficient time to adjust to silylation and oxidation reactions on the surface of zeolites, the crystals not agglomerate, and the modified zeolites system was lower energy and more stable.

Figure 3 shows the IR spectra of the original HYX (X = 5.40) and the zeolites modified by Organosilanes and Vapor phase silanization overlay modification, the peak at 584.69 cm^{-1} corresponds to the double ring external linkage vibration, which corresponds to the double hexa ring structure of Y zeolites, 1075 cm^{-1} corresponds to the Si-O stretching vibration, 820 cm^{-1} corresponds to the Al-O-Si vibration. It can be seen that the characteristic vibrational peaks of

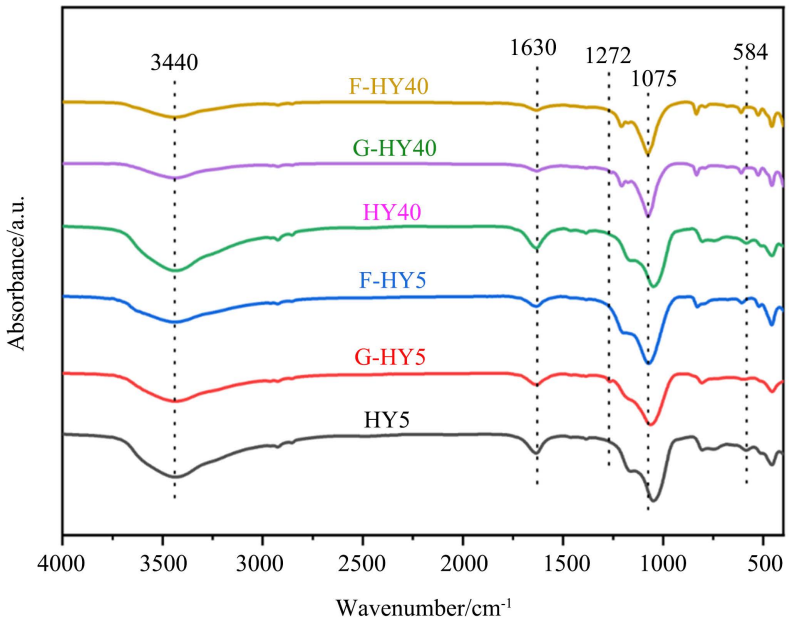

Figure 3. IR diagram of Y zeolites.

the zeolites skeleton did not change significantly before and after the modification, and neither Organosilanes , nor Vapor phase silanization overlay modification changed the zeolites skeleton structure. The absorption peak near 1630 cm^{-1} corresponds to the variable angle vibration peak that absorbs water, and the absorption peak near 3440 cm^{-1} corresponds to the expansion vibration peak of the hydroxyl group. From the zeolites map of HY5 and HY40, it can be seen that the absorption peak was widened and the strength of the absorption peak was large, which may be unmodified and hydrothermal dealuminum-modified Y zeolites surface with a large silicon hydroxyl density or hydrogen bonds that absorb water [38] [39]. The amount of water-absorbing site -OH of G-HYX (X = 5.40) zeolites was reduced after silanization modification, and the absorption peak of stretching vibration of Si-CH_3 bond at 1260 cm^{-1}; the small peak at 1272.81 cm^{-1} was caused by the vibration of Si-C, and the intensity of hydroxyl absorption peak corresponding to 3300 - 3500 cm^{-1} was weakened, which indicates that the silanization modification successfully grafted carbon silane groups on the surface of Y zeolites. The "Si-OH group" formed by the zeolitic aluminum cavities on the surface of Y zeolites with terminal Si-OH, amorphous Al-OH, and acidic Al-OH located at different positions of the skeleton can be condensed with TMCS due to the terminal silicon hydroxyl group, forming -$OSi(CH_3)_3$ or -$OSi(CH_3)_2$ hydrophobic carbosilane groups on the surface of the zeolites, so the intensity of the G-HYX (X = 5.40) zeolites hydroxyl absorption peak and the vibration peak of absorbing water becomes weaker. Due to the oxidation, the peaks of the hydrophobic Si-CH_3 bond disappeared after the silylation modification, however, the intensity of the hydroxyl absorption peak and the vibrational peak of the absorbing water remained almost unchanged compared with the silylation. The reason for this was that the directional mass transfer effect of sila-

nization causes the formation of hydrophobic silica surface around the hydroxyl group in the water absorption site of Y zeolites, which affects the hydroxyl absorption peak and leads to the weakening of the hydroxyl absorption peak and the vibration peak of water absorption.

From **Figure 4**, the basic structural unit of Y zeolites was composed of silicon and aluminum atoms TO_4 tetrahedra, depending on the number of AlO_4 tetrahedra linking SiO_4 tetrahedra, there are five different environments of silicon Si (nAl) in the structural unit (n is the number of aluminum atoms in the coordination tetrahedron, n can be 0, 1, 2, 3 or 4). In **Figure 4**, there are five different chemical displacements, $\delta = -84, -85, -87, -91$ and -93, they belong to Si (4Al), Si (3Al), Si (2Al) and Si (0Al) structural units respectively. Resonance peaks appear at $\delta = -79, -80, -82, -90$, corresponding to Q^1 ($SiOSi^*\text{-}(OH)_3$), Q^2 ($(SiO)_2Si^*\text{-}(OH)_2$), Q^3 ($(SiO)_3Si^*\text{-}OH$), Q^4 ($(SiO)_4Si^*$) (Q denotes Si connected through four O atoms) silicon species at different positions in the backbone [40]. After silylation, the reaction of the silane reagent with part of the Q^3 species in HY5, HY40 resulted in a weakening of the resonance peak at $\delta = -82.3$ and a new peak at $\delta = -77.7$ in G-HY5, G-HY40, which should be attributed to $(SiO)_3Si\text{-}OSi^*(CH_3)_3$, indicating that the carbon silane group has been grafted to the surface of the specimen. The resonance peak corresponding to the $(SiO)_3Si\text{-}OSi^*(CH_3)_3$ species disappears after Vapor phase silanization overlay modification, while the signal peak of Q^4 species appears at $\delta = -90.2$, which was attributed to the amorphous SiO_2 species and was the vibrational peak of the Si species of the new environment generated by the oxidation of trimethylsilane grafted to the surface of the zeolites. The shift of the peak position toward the high field (HYX zeolites peak tip at −83.89 and F-HYX at 84.41) after the Vapor phase silanization overlay modification was due to the diffusion of the carbon silane fragments from the oxygen gas stream into the solid and the formation of crystals with the active Si in the solid, where more SiO_2 tetrahedra were connected in the crystal layer leading to the shift toward the high field.

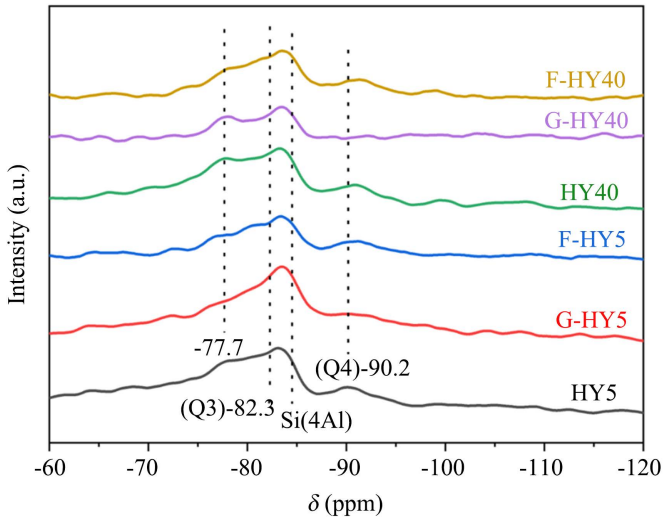

Figure 4. ^{29}Si NMR diagram of Y zeolites.

The pore structure characteristics before and after Y zeolites modification calculated according to the results of N_2 adsorption isotherm were listed in Table 1. After silylation, the specific surface area and pore volume of GHY-X (X = 5.40) were significantly reduced compared with the original Y zeolites, but still showed a rich pore structure. The specific surface area changed significantly before and after silylation, but the pore size did not change much and remained in the micropore range [41]. The main reason was the condensation reaction between TMCS and Si-OH groups on the surface of zeolites, which leads to the grafting of $-Si(CH_3)_3$ or $-Si(CH_3)_2$ groups on the inner surface of zeolites pore channels. At the same time, the more the number of methyl CH_3 in chlorosilane, the more significant the spatial resistance formed by the silylation products, which leads to the reduction of specific surface area, pore volume and pore diameter. The pore size of Y zeolites modified with silane remained the same, and the specific surface area decreased slightly, indicating that the oxidation of silyl groups grafted on the surface of Y zeolites to SiO_2 transcrystallized on the surface of zeolites, forming a hydrophobic surface, avoiding the blockage of pore channels of zeolites by grafted long carbon chains, reducing the adsorption capacity of VOCs, and achieving hydrophobic modification (without destroying the basic structure of zeolites) while maintaining the adsorption capacity of VOCs. The zeolites can be used to reduce the hydrophobic modification (without destroying the basic structure of the zeolites) while maintaining the adsorption capacity of VOCs.

The SEM analysis by Figure 5 revealed that the unmodified Y zeolites skeleton particles are loosely distributed and nanoporous material with continuous network structure, while the hydrophobically modified Y zeolites was microporous material with nanoparticle composition, and the hydrophobically modified zeolites surface grafted with carbon silane groups will occupy part of the internal pore channels, while shaping the rough surface of nanometer size with very dense distribution and uniform particles.

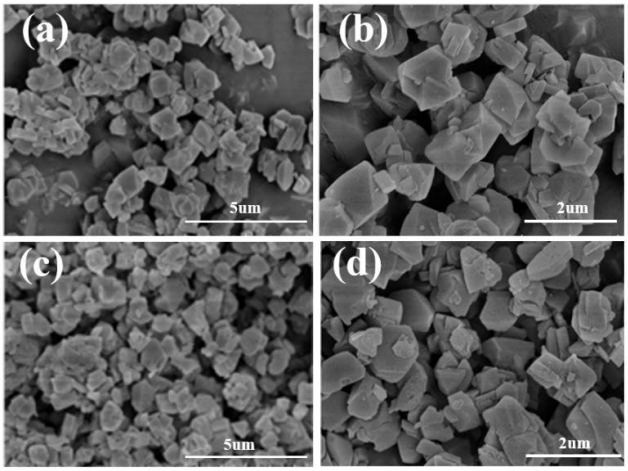

Figure 5. SEM diagram of Y zeolites ((a) and (b): before modification; (c) and (d): after modification).

Table 1. Pore structure characteristics of zeolites before and after modification.

Materials	$S_{BET}/(m^2 \cdot g^{-1})$	$S_{Mic}/(m^2 \cdot g^{-1})$	$S_{EXt}/(m^2 \cdot g^{-1})$	$V_{Tol}/(ml \cdot g^{-1})$	Pore Diameter/nm
HY-5	945	863	82	0.52	1.72
GHY-5	756	684	72	0.41	1.12
FHY-5	869	790	79	0.51	1.69
HY-40	912	839	73	0.56	1.92
GHY-40	763	699	64	0.46	1.32
FHY40	865	794	71	0.54	1.91

Note: S_{BET}: BET surface area obtained from N_2 adsorption isotherm; S_{Mic}: micropore surface area; S_{Ext}: external surface area; V_{Tol}: total pore volume; V_{Tol}, S_{mic} and S_{Ext} are obtained from the t-plot method.

The water contact angle test results of zeolites samples before and after silicon coating modification were shown in **Figure 6**. For the unmodified HY5 zeolites, the water droplets were instantly drawn into the zeolites pore channel in contact with the surface of the zeolites with a contact angle of 0˚, and the static water contact angle of the HY40 zeolites was 82˚, indicating that the zeolites has a strong hydrophilicity. The silicon-aluminum ratio of HY40 zeolites prepared by hydrothermal composite treatment was further improved, but a large number of terminal silicon hydroxyl groups were still hydrophilic after dealumination. These Si-OH groups were also hydrophilic centres like cations, so the simple dealumination hydrophobic effect was limited. The static water contact angle of the silicon-modified F-HYX (X = 5.40) zeolites was 106˚ and 121˚ respectively, indicating the hydrophobicity of the zeolites surface was enhanced.. Nanoscale hydrophobic surfaces were formed on the zeolites surface, and the oxygen atoms in this Si-O-Si bond were not basic and do not form hydrogen bonds, so the adsorbed micropores were surrounded by nonpolar oxygen atoms and exhibit hydrophobic properties [42] [43].

The results of the saturated water absorption rate of Y zeolites under different humidity were shown in **Figure 7**, which shows that the hydrophobicity of Y zeolites has been significantly improved after the modification of silicon. With the increase of relative humidity, compared with the unmodified Y zeolites, the saturated water absorption rate of Y zeolites after modification grows slowly and always remains below 10%, which can prove that the hydrophobic effect of the modified zeolites was better.

As shown in **Figure 8**, the dynamic adsorption curves of HYX (X = 5.40) and F-HYX (X = 5.40) were basically the same. Under the condition of RH = 0%, when the mass concentration of toluene in the air intake was low, the balanced adsorption amount of toluene increases rapidly after adsorption penetration, which was a typical microporous adsorption phenomenon. The HY zeolites has an intrinsic microporous structure. Its microporous wall has a strong adsorption

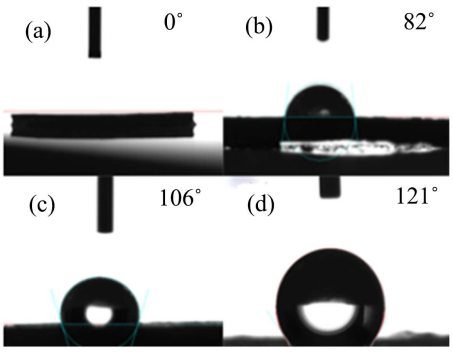

Figure 6. The water contact angle test results diagram of Y zeolites ((a)-HY5, (b)-HY40, (c)-F-HY5, (d)-F-HY40).

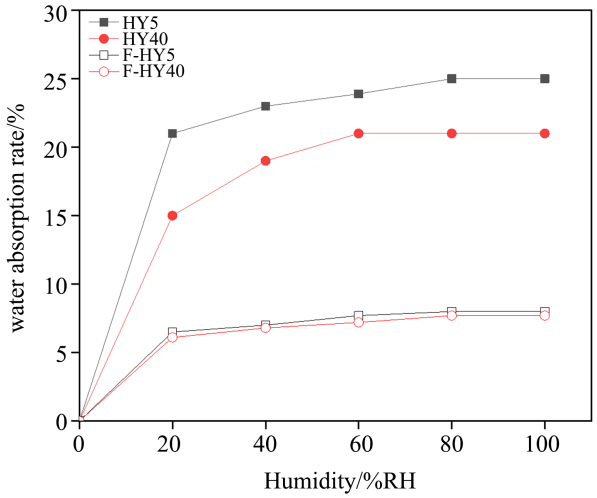

Figure 7. Saturated water absorption rate at different humidity of Y zeolites.

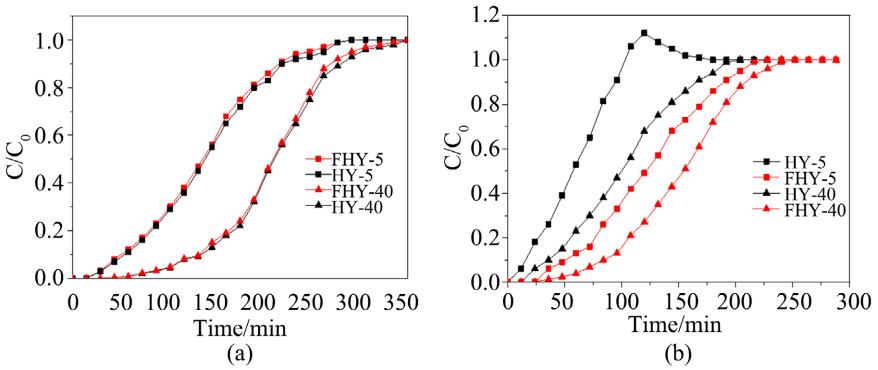

Figure 8. Dynamic adsorption curve of Y zeolites ((a): RH = 0%; (b): RH = 60%).

effect on toluene molecules, causing toluene molecules to quickly fill the micropores of HY zeolites. Subsequently, the adsorption rate decreases significantly and the adsorption amount slowly increases, indicating that the micropores of the zeolites sample to the single layer adsorption of toluene was saturated. HY zeolites particles accumulate to form mesopores and multi-layer adsorption occurs, so the adsorption of toluene was relatively slow. As can be seen from Table 2,

Table 2. Y zeolites dynamic adsorption performance.

Materials	RH = 0%			RH = 60%			
	Eav/(g·g^{-1})	t_p/(min)	Tsac/(g·g^{-1})	Eav/(g·g^{-1})	t_p/(min)	Tsac/(g·g^{-1})	Wsac/(g·g^{-1})
HY-5	0.18	45	0.21	0.04	18	0.06	0.16
FHY-5	0.17	44	0.20	0.11	41	0.15	0.05
HY-40	0.25	135	0.29	0.07	35	0.09	0.21
FHY-40	0.24	133	0.28	0.18	79	0.21	0.07

Note: GHSV = 15,000 ml·h^{-1}·g^{-1}, T = 35˚C, C_0 = 5000 mg·m^{-3}, Eav: End adsorption volume, t_p: penetration time, Tsac: toluene saturation adsorption capacity, Wsac: water saturation adsorption capacity.

under 60% RH when organic matter and water vapor together into the Y zeolites system, unmodified Y zeolites showed strong selective adsorption of polar water molecules, HYX (X = 5.40) toluene saturation adsorption decreased by 72%, 69%, respectively, while F-HYX (X = 5.40) by water vapor influence was small, toluene saturation adsorption only slightly decreased. Among them, after zeolites adsorption saturation occurs during the adsorption process of HY5 zeolites, toluene was partially replaced by water molecules. Figure 8 shows that C/C_0 was greater than 1 in the penetration curve, because H^+ produces hydrogen bonds with water molecules, thus replacing the adsorbed toluene. The failure of HY40 was mainly because the hydrothermal reaction increases the silicon-aluminum ratio of the zeolites, the number of cationic H^+ to compensate the charge decreases, and the interaction force with water was reduced, showing a certain hydrophobicness.

4. Conclusion

In this experiment, the zeolites surface and pores were modified by TMCS with polar terminal groups, the terminal silica hydroxyl groups exposed under high temperature were condensed with highly reactive carbon silane fragments formed by pyrolysis, and the silyl methyl groups were grafted on the zeolites surface under the action of oxygen. The hydrophobicity of the silica-modified zeolites surface was enhanced, which not only covers the hydrophilic sites, but also ensures that the zeolite structure and thermal stability were not changed. Compared with the silylation modification, the Vapor phase silanization overlay modified zeolites was enhanced while its adsorption performance on toluene remains almost unchanged. This experiment provides methods and ideas for the modification process of zeolites, which makes the study of high humidity application of zeolites more valuable.

Conflicts of Interest

The authors declare no conflicts of interest regarding the publication of this paper.

References

[1] Meng, X.J. and Xiao, F.S. (2014) Green Routes for Synthesis of Zeolites. *Chemical Reviews*, **114**, 1521-1543. https://doi.org/10.1021/cr4001513

[2] Hosseini, M., Zanjanchi, M.A., Ghalami-Choobar, B. and Golmojdeh, H. (2015) Ultrasound-Assisted Dealumination of Zeolite Y. *Journal of Chemical Sciences*, **127**, 25-31. https://doi.org/10.1007/s12039-014-0745-2

[3] Jal, P.K., Patel, S. and Mishra, B.K. (2004) Chemical Modification of silica Surface by Immobilization of Functional Groups for Extractive Concentration of Metal Ions. *Talanta*, **62**, 1005-1028. https://doi.org/10.1016/j.talanta.2003.10.028

[4] Zheng, H.M., Zhao, L. and Yang, Q. (2016) Insight into the Adsorption Mechanism of Benzene in HY Zeolites: The Effect of Loading. *RSC Advances*, **6**, 34175-34187. https://doi.org/10.1039/C6RA02338J

[5] Kimura, T., Suzuki, M., Maeda, M. and Tomura, S. (2006) Water Adsorption Behavior of Ordered Mesoporous Silicas Modified with an Organosilane Composed of Hydrophobic Alkyl Chain and Hydrophilic Polyethylene Oxide Groups. *Microporous and Mesoporous Materials*, **95**, 213-219. https://doi.org/10.1016/j.micromeso.2006.05.027

[6] Gola, A., *et al.* (2000) Effect of Leaching Agent in the Dealumination of Stabilized Y Zeolites. *Microporous and Mesoporous Materials*, **40**, 73-83. https://doi.org/10.1016/S1387-1811(00)00243-2

[7] Kuwahara, Y., Kamegawa, T., Mori, K. and Yamashita, H. (2008) Fabrication of Hydrophobic Zeolites Using Triethoxyfluorosilane and Their Application as Supports for TiO_2 Photocatalysts. *Chemical Communications*, No. 39, 4783-4785. https://doi.org/10.1039/b810053e

[8] Baek, S.W., Kim, J.R. and Ihm, S.K. (2004) Design of Dual Functional Adsorbent/Catalyst System for the Control of VOC's by Using Metal-Loaded Hydrophobic Y-Zeolites. *Catalysis Today*, **93**, 575-581. https://doi.org/10.1016/j.cattod.2004.06.107

[9] Parmar, G.R. and Rao, N.N. (2009) Emerging Control Technologies for Volatile Organic Compounds. *Critical Reviews in Environmental Science and Technology*, **39**, 41-78. https://doi.org/10.1080/10643380701413658

[10] Ye, QQ., Chen, Y.Y., Li, Y.Z., Jin, R.B., Geng, Q. and Chen, S. (2023) Management of Typical VOCs in Air with Adsorbents: Status and Challenges. *Dalton Transactions*, **52**, 12169-12184. https://doi.org/10.1039/D3DT01930F

[11] Meininghaus, C.K. and Prins, R. (2000) Sorption of Volatile Organic Compounds on Hydrophobic Zeolites. *Microporous and Mesoporous Materials*, **35**, 349-365. https://doi.org/10.1016/S1387-1811(99)00233-4

[12] Serrano, D.P., Calleja, G., Botas, J.A. and Gutierrez, F.J. (2004) Adsorption and Hydrophobic Properties of Mesostructured MCM-41 and SBA-15 Materials for Volatile Organic Compound Removal. *Industrial & Engineering Chemistry Research*, **43**, 7010-7018. https://doi.org/10.1021/ie040108d

[13] Serrano, D.P., Calleja, G., Botas, J.A. and Gutierrez, F.J. (2007) Characterization of Adsorptive and Hydrophobic Properties of Silicalite-1, ZSM-5, TS-1 and β Zeolites by TPD Techniques. *Separation and Purification Technology*, **54**, 1-9. https://doi.org/10.1016/j.seppur.2006.08.013

[14] Stelzer, J., Paulus, M., Hunger, M. and Weitkamp, J. (1998) Hydrophobic Properties of All-Silica Zeolite β. *Microporous and Mesoporous Materials*, **22**, 1-8. https://doi.org/10.1016/S1387-1811(98)00071-7

[15] Martucci, A., *et al.* (2015) Influence of Water on the Retention of Methyl Tertiary-Butyl Ether by High Silica ZSM-5 and Y Zeolites: A Multidisciplinary Study on the Adsorption from Liquid and Gas Phase. *RSC Advances*, **5**, 86997-87006. https://doi.org/10.1039/C5RA15201A

[16] Han, X., Wang, L., Li, J., Zhan, X., Chen, J. and Yang, J. (2011) Tuning the Hydrophobicity of ZSM-5 Zeolites by Surface Silanization Using Alkyltrichlorosilane. *Applied Surface Science*, **257**, 9525-9531. https://doi.org/10.1016/j.apsusc.2011.06.054

[17] Zhao, X.S. and Lu, G.Q. (1998) Modification of MCM-41 by Surface Silylation with Trimethylchlorosilane and Adsorption Study. *The Journal of Physical Chemistry B*, **102**, 1556-1561. https://doi.org/10.1021/jp972788m

[18] Kim, K.J. and Ahn, H.G. (2012) The Effect of Pore Structure of Zeolite on the Adsorption of VOCs and Their Desorption Properties by Microwave Heating. *Microporous and Mesoporous Materials*, **152**, 78-83. https://doi.org/10.1016/j.micromeso.2011.11.051

[19] Hung, C., Bai, H. and Karthik, M. (2009) Ordered Mesoporous Silica Particles and Si-MCM-41 for the Adsorption of Acetone: A Comparative Study. *Separation and Purification Technology*, **64**, 265-272. https://doi.org/10.1016/j.seppur.2008.10.020

[20] Pasti, L., Martucci, A., Nassi, M., Cavazzini, A., Alberti, A. and Bagatin, R. (2012) The Role of Water in DCE Adsorption from Aqueous Solutions onto Hydrophobic Zeolites. *Microporous and Mesoporous Materials*, **1600**, 182-193. https://doi.org/10.1016/j.micromeso.2012.05.015

[21] Yu, Y., Zheng, L. and Wang, J. (2012) Adsorption Behavior of Toluene on Modified 1X Molecular Sieves. *Journal of the Air & Waste Management Association*, **62**, 1227-1232. https://doi.org/10.1080/10962247.2012.702186

[22] Martucci, A., Braschi, I., Bisio, C., Sarti, E., Rodeghero, E., Bagatin, R. and Pasti, L. (2015) Influence of Water on the Retention of Methyl *Tertiary*-Butyl Ether by High Silica ZSM-5 and Y Zeolites: A Multidisciplinary Study on the Adsorption from Liquid and Gas Phase. *RSC Advances*, **106**, 86997-87006. https://doi.org/10.1039/C5RA15201A

[23] Halasz, I., Kim, S. and Marcus, B. (2002) Hydrophilic and Hydrophobic Adsorption on Y Zeolites. *Molecular Physics*, **19**, 3123-3132. https://doi.org/10.1080/00268970210133198

[24] Dabbawala, A.A., Reddy, K.S.K., Mittal, H., Al Wahedi, Y., Vaithilingam, B.V., Karanikolos, G.N., Singaravel, G., Morin, S., Berthod, M. and Alhassan, S.M. (2021) Water Vapor Adsorption on Metal-Exchanged Hierarchical Porous Zeolite-Y. *Microporous and Mesoporous Materials*, **326**, Article ID: 111380. https://doi.org/10.1016/j.micromeso.2021.111380

[25] Jin, W. and Zhu, S. (2000) Study of Adsorption Equilibrium and Dynamics of Benzene, Toluene, and Xylene on Zeolite NaY. *Chemical Engineering & Technology*, **23**, 151-156.

[26] Zhu, J., Trefiak, N., Woo, T. and Huang, Y. (2008) An Investigation of the Adsorption of Aromatic Hydrocarbons in Zeolite Na-Y by Solid-State NMR Spectroscopy. *Microporous and Mesoporous Materials*, **114**, 474-484. https://doi.org/10.1016/j.micromeso.2008.01.035

[27] Zhu, J., Mosey, N., Woo, T. and Huang, Y. (2007) Study of the Adsorption of Toluene in Zeolite LiNa-Y by Solid-State NMR Spectroscopy. *The Journal of Physical Chemistry C*, **111**, 13427-13436. https://doi.org/10.1021/jp0706275

[28] Canet, X., Gilles, F., Su, B.L., de Weireld, G., Frère, M. and Mougin, P. (2007) Adsorption of Alkanes and Aromatic Compounds on Various Faujasites in the Henry

Domain. 2. Composition Effect in X and Y Zeolites. *Journal of Chemical & Engineering Data*, **52**, 2127-2137. https://doi.org/10.1021/je700214v

[29] Kondor, A. and Dallos, A. (2014) Adsorption Isotherms of Some Alkyl Aromatic Hydrocarbons and Surface Energies on Partially Dealuminated Y Faujasite Zeolite by Inverse Gas Chromatography. *Journal of Chromatography A*, **1362**, 250-261. https://doi.org/10.1016/j.chroma.2014.08.047

[30] Rungsirisakun, R., Nanok, T., Probst, M. and Limtrakul, J. (2006) Adsorption and Diffusion of Benzene in the Nanoporous Catalysts FAU, ZSM-5 and MCM-22: A Molecular Dynamics Study. *Journal of Molecular Graphics and Modelling*, **24**, 373-382. https://doi.org/10.1016/j.jmgm.2005.10.003

[31] Plant, D.F., Maurin, G. and Bell, R.G. (2007) Diffusion of Methanol in Zeolite NaY: A Molecular Dynamics Study. *The Journal of Physical Chemistry B*, **111**, 2836-2844. https://doi.org/10.1021/jp0674524

[32] Smit, B. and Maesen, T.L. (2008) Molecular Simulations of Zeolites: Adsorption, Diffusion, and Shape Selectivity. *Chemical Reviews*, **108**, 4125-4184. https://doi.org/10.1021/cr8002642

[33] Zheng, S., Tanaka, H., Jentys, A. and Lercher, J.A. (2004) Novel Model Explaining Toluene Diffusion in HZSM-5 after Surface Modification. *The Journal of Physical Chemistry B*, **108**, 1337-1343. https://doi.org/10.1021/jp034477j

[34] Malka-Edery, A. and Grenier, P. (2001) Diffusion of Benzene in NaX Zeolite, Studied by Thermal Frequency Response. *The Journal of Physical Chemistry B*, **105**, 6853-6857. https://doi.org/10.1021/jp004025w

[35] Takeuchi, M., Hidaka, M. and Anpo, M. (2014) Simple Evaluation of the Adsorption States of Benzene Molecule on the Hydroxyl, H^+ and Na^+ Sites of Y-Zeolite Surfaces by Using UV Absorption Spectroscopy. *Research on Chemical Intermediates*, **40**, 2315-2325. https://doi.org/10.1007/s11164-014-1608-7

[36] Halasz, I., Kim, S. and Marcus, B. (2002) Hydrophilic and Hydrophobic Adsorption on Y Zeolites. *Molecular Physics*, **100**, 3123-3132. https://doi.org/10.1080/00268970210133198

[37] Chaouati, N., Soualah, A. and Chater, M. (2013) Adsorption of Phenol from Aqueous Solution onto Zeolites Y Modified by Silylation. *Comptes Rendus Chimie*, **16**, 222-228. https://doi.org/10.1016/j.crci.2012.10.010

[38] Tsai, W.T., Hsu, H.C., Su, T.Y., Lin, K.Y. and Lin, C.M. (2006) Adsorption Characteristics of Bisphenol-A in Aqueous Solutions onto Hydrophobic Zeolite. *Journal of Colloid and Interface Science*, **299**, 513-519. https://doi.org/10.1016/j.jcis.2006.02.034

[39] Guillemot, M., Mijoin, J., Mignard, S. and Magnoux, P. (2008) Adsorption of Tetrachloroethylene (PCE) in Gas Phase on Zeolites of Faujasite Type: Influence of Water Vapour and of Si/Al Ratio. *Microporous and Mesoporous Materials*, **111**, 334-342. https://doi.org/10.1016/j.micromeso.2007.08.035

[40] Cheng, H. and Reinhard, M. (2007) Sorption and Inhibited Dehydrohalogenation of 2, 2-Dichloropropane in Micropores of Dealuminated Y Zeolites. *Environmental Science & Technology*, **41**, 1934-1941. https://doi.org/10.1021/es062332v

[41] Guillemot, M., Mijoin, J., Mignard, S. and Magnoux, P. (2007) Adsorption of Tetrachloroethylene on Cationic X and Y Zeolites: Influence of Cation Nature and of Water Vapor. *Industrial & Engineering Chemistry Research*, **46**, 4614-4620. https://doi.org/10.1021/ie0616390

[42] Pires, J., Carvalho, A., Veloso, P. and de Carvalho, M.B. (2002) Preparation of Dea-

luminated Faujasites for Adsorption of Volatile Organic Compounds. *Journal of Materials Chemistry*, **12**, 3100-3104. https://doi.org/10.1039/b205367e

[43] Sakuth, M., Meyer, J. and Gmehling, J. (1995) Vapor Phase Adsorption Equilibria of Toluene+1-Propanol Mixtures on Y-Zeolites with Different Silicon to Aluminum Ratios. *Journal of Chemical and Engineering Data*, **40**, 895-899. https://doi.org/10.1021/je00020a035